J Biol Inorg Chem (2004) 9: 354–364
DOI 10.1007/s00775-004-0531-6

ORIGINAL ARTICLE

**Anna C. G. Hotze · Sabrine E. Caspers · Dick de Vos
Huub Kooijman · Anthony L. Spek · Anna Flamigni
Marina Bacac · Gianni Sava · Jaap G. Haasnoot
Jan Reedijk**

Structure-dependent in vitro cytotoxicity of the isomeric complexes $[Ru(L)_2Cl_2]$ (L=*o*-tolylazopyridine and 4-methyl-2-phenylazopyridine) in comparison to $[Ru(azpy)_2Cl_2]$

Received: 12 November 2003 / Accepted: 14 February 2004 / Published online: 19 March 2004

Abstract The dichlorobis(2-phenylazopyridine)ruthenium(II) complexes, $[Ru(azpy)_2Cl_2]$, are under renewed investigation due to their potential anticancer activity. The three most common isomers α-, β- and γ-$[RuL_2Cl_2]$ with L = *o*-tolylazopyridine (tazpy) and 4-methyl-2-phenylazopyridine (mazpy) (α indicating the coordinating Cl, N(pyridine) and Nazo atoms in mutual *cis*, *trans*, *cis* positions, β indicating the coordinating Cl, N(pyridine) and Nazo atoms in mutual *cis*, *cis*, *cis* positions, and γ indicating the coordinating Cl, N(pyridine) and Nazo atoms in mutual *trans*, *cis*, *cis* positions) are synthesized and characterized by NMR spectroscopy. The molecular structures of γ-$[Ru(tazpy)_2Cl_2]$ and α-$[Ru(mazpy)_2Cl_2]$ are determined by X-ray diffraction analysis. The IC_{50} values of the geometrically isomeric $[Ru(tazpy)_2Cl_2]$ and $[Ru(mazpy)_2Cl_2]$ complexes compared with those of the parent $[Ru(azpy)_2Cl_2]$ complexes are determined in a series of human tumour cell lines (MCF-7, EVSA-T, WIDR, IGROV, M19, A498 and H266). These data unambiguously show for all complexes the following trend: the α isomer shows a very high cytotoxicity, whereas the β isomer is a factor 10 less cytotoxic. The γ isomers of $[Ru(tazpy)_2Cl_2]$ and $[Ru(mazpy)_2Cl_2]$ display a very high cytotoxicity comparable to that of the γ isomer of the parent compound $[Ru(azpy)_2Cl_2]$ and to that of the α isomer. These biological data are of the utmost importance for a better understanding of the structure–activity relationships for the isomeric $[RuL_2Cl_2]$ complexes.

Keywords Ruthenium(II) complexes · 2-Phenylazopyridine-like ligands · NMR spectroscopy · Cytotoxicity · Cellular uptake

Abbreviations *AAS* atomic absorption spectroscopy · *azpy* 2-phenylazopyridine · *COSY* correlation spectroscopy · *mazpy* 4-methyl-2-phenylazopyridine · *MTT* 3-(4,5-dimethylthiazol-2-yl)-2,5-diphenyl-2H-tetrazolium bromide · *NOESY* nuclear Overhauser-effect spectroscopy · *PBS* phosphate-buffered saline · *tazpy* *o*-tolylazopyridine

Introduction

Several ruthenium complexes are known for their capacity to control tumour proliferation, growth and metastasis in preclinical models [1, 2, 3]. These complexes are characterized by a number of different ligands, different geometries and various oxidation states. For this reason, no general structure–activity relationships (SARs) for anticancer ruthenium complexes have been developed yet. Based on cisplatin and analogous compounds, one of the most important SARs of antitumour-active platinum complexes is the presence of

Electronic Supplementary Material Supplementary material is available in the online version of this article at http://dx.doi.org/10.1007/s00775–004–0531–6.

A. C. G. Hotze · S. E. Caspers · J. G. Haasnoot · J. Reedijk (✉)
Leiden Institute of Chemistry, Gorlaeus Laboratories,
Leiden University, P.O. Box 9502, 2300 RA Leiden,
The Netherlands
E-mail: reedijk@chem.leidenuniv.nl
Tel.: +31-71-5274459
Fax: +31-71-5274671

D. de Vos
Pharmachemie BV, P.O. Box 552, 2003 RN Haarlem,
The Netherlands

H. Kooijman · A. L. Spek
Bijvoet Center for Biomolecular Research,
Crystal and Structural Chemistry, Utrecht University,
Padualaan 8, 3584 CH Utrecht, The Netherlands

A. Flamigni · M. Bacac · G. Sava
Department of Biomedical Sciences, University of Trieste,
via L. Giorgieri 7, 34127 Trieste, Italy

M. Bacac · G. Sava
Callerio Foundation Onlus, via A. Fleming 22–31,
34127 Trieste, Italy

two labile *cis*-coordinated (chloride) ligands [4, 5]. A logical step to take in anticancer ruthenium chemistry has been the development of ruthenium complexes with two labile *cis*-coordinated chloride ligands. However, one should also consider the fact that ruthenium is octahedrally coordinated in the two most common oxidation states, +2 and +3, whereas platinum is square planar. This difference might have important consequences for the interaction with biomolecules and thus biological activity.

The $[RuL_2Cl_2]$ type of complexes with two chelating polypyridyl ligands, L, which are not likely to dissociate, and two *cis*-chloro ligands are an interesting group of complexes to investigate for anticancer properties. The $[RuL_2Cl_2]$ complexes with L = 2,2′-bipyridine or phenanthroline do not show any significant effect on tumour cells in vitro [6, 7]. Surprisingly, the related, but sterically quite different, bis-chelated $[Ru(azpy)_2Cl_2]$ complexes (azpy = 2-phenylazopyridine) do show cytotoxic activity [8]. The ligand 2-phenylazopyridine is an asymmetric ligand; for this reason, the dichlorobis(2-phenylazopyridine)ruthenium(II) complexes, $[Ru(azpy)_2Cl_2]$, can theoretically exist in five different isomeric forms (Fig. 1).

Three isomers, i.e. the so-called α, β and γ isomers (α indicates the coordinating pairs Cl, Npy and Nazo in mutual *cis*, *trans*, *cis* positions; β means coordinating atoms Cl, Npy, Nazo *cis*, *cis*, *cis;* and γ means coordinating atoms Cl, Npy, Nazo *trans*, *cis*, *cis*) are the most common ones, and were already discovered in the early 1980s [9, 10]. One of the isomers had been characterized erroneously, i.e. the γ isomer was originally identified as the all-*trans* isomer (coordinating chloride, Npy and Nazo atoms in mutual *trans* position). However, recent X-ray investigations of the structure of the γ isomer have unambiguously shown the configuration of this isomer: the Cl ligands are in a *trans* position, but the pyridine and azo nitrogen atoms are mutually *cis*-coordinated [8]. The fourth newly discovered so-called delta isomer has been reported to be the all-*trans* isomer, and a thorough characterization of the four isomers, i.e. α, β, γ and δ-$[Ru(azpy)_2Cl_2]$ is now available [11]. The synthesis of the fifth isomer, ϵ-$[Ru(azpy)_2Cl_2]$ (Cl and Npy atoms *cis*, Nazo atoms *trans*), has been mentioned in the literature, but no clear NMR characterization and/or X-ray structure determination has been reported, and the configuration was proven only by spectrophotometric data [12].

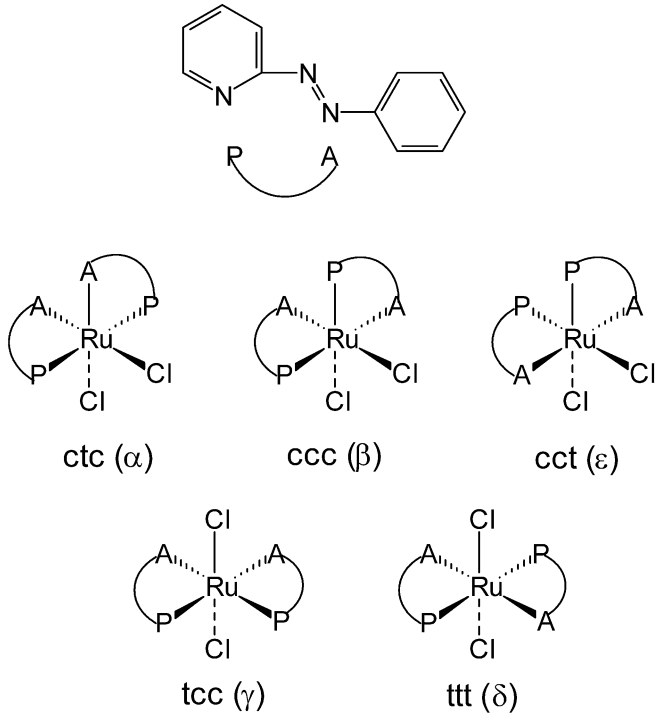

Fig. 1 Structural representation *(above)* of the didentate ligand azpy and schematic representation *(below)* of the five possible $[Ru(azpy)_2Cl_2]$ isomers. The *three-letter code* indicates the mutual *cis* (c) or *trans* (t) orientation of the chlorides (Cl), the pyridine (Npy) and the azo nitrogens (Nazo), respectively. The *Greek letter code* is given between brackets, and is used throughout this paper

The α, β and γ-$[Ru(azpy)_2Cl_2]$ isomers (Fig. 1) have been tested for their cytotoxicity in the panel of cell lines MCF-7, EVSA-T, WIDR, IGROV, M19, A498 and H266 [8]. The α-isomer, α-$[Ru(azpy)_2Cl_2]$, has been reported to show a remarkably high cytotoxicity, even more pronounced than cisplatin in most of the tested cell lines [8]. Noteworthy is the difference in cytotoxicity between the two *cis* isomers (Fig. 1), α and β, of which the latter shows a cytotoxicity of a factor of 10 lower than the α isomer in the same panel of cell lines, and the *trans* isomer, γ, being devoid of any cytotoxic effect [8].

To further confirm and investigate the cytotoxic activity of the dichlorobis(2-phenylazopyridine)ruthenium(II) complexes, two methylated azpy ligands have been synthesized, i.e. *o*-tolylazopyridine (tazpy) and 4-methyl-2-phenylazopyridine (mazpy), and the respective ruthenium compounds and their isomers have been prepared consecutively (Fig. 2). Although methylated azpy ligands have already been described [9, 13, 14], no X-ray structure determinations of dichlorobis(methylazpy)ruthenium(II)complexes with tazpy or mazpy ligands have been reported yet. To our knowledge, the only molecular structure of a bis-chelated ruthenium complex with a methylated azpy ligand is of the compound catecholatobis(2-(*m*-tolylazo)pyridine)ruthenium (II) [15]. The ligand 4-methyl-2-phenylazopyridine has been shown to be associated in molybdenum and iron complexes [16,17].

As a thorough structural characterization of the parent complexes α, β, γ and δ-$[Ru(azpy)_2Cl_2]$ has recently been reported [11], we will focus now on the differences in structural aspects caused by the added methyl group. Moreover, by adding new data on the effects on tumour cell proliferation of these methylated azpy complexes, we will reconsider the cytotoxic activity of $[RuL_2Cl_2]$ complexes (L = azpy, tazpy and mazpy).

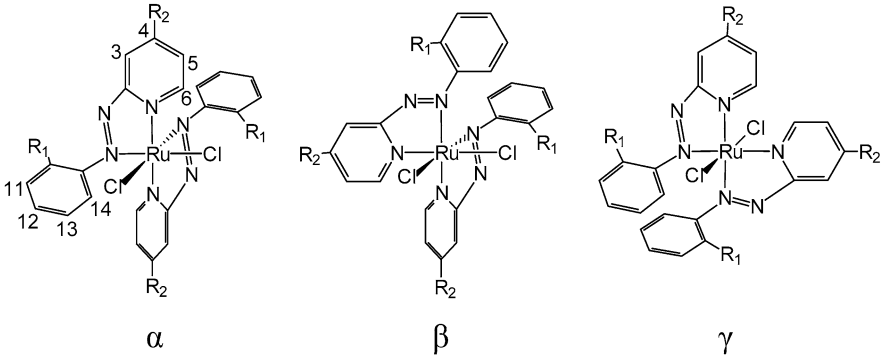

Fig. 2 Representation of the three most common isomers, i.e. α, β and γ of the $[RuL_2Cl_2]$ complexes with L = 2-phenylazopyridine (azpy), 4-methyl-2-phenylazopyridine (mazpy) and *o*-tolylazopyridine (tazpy), and numbering used for the NMR assignment

Materials and Methods

Materials

The ligand *o*-tolylazopyridine (tazpy) has been synthesized according to the synthesis [10] of 2-phenylazopyridine using nitrosotoluene instead of nitrosobenzene. 4-Methyl-2-phenylazopyridine (mazpy) has also been synthesized according to the synthesis of 2-phenylazopyridine using 4-methyl-2-aminopyridine instead of 2-aminopyridine. For purification of β-$[Ru(mazpy)_2Cl_2]$ (complex **6**), neutral alumina (ICN AluminaN Akt. 1) was used. The structures of the ligands are depicted in Fig. 2.

The complexes **1–6** were prepared by using general procedures according to the literature [9, 10, 18]. Details are given for complexes **1–3** below, and complexes **4–6** were synthesized according to the same procedures.

Syntheses

γ-[Ru(tazpy)$_2$Cl$_2$] (complex **1***)*

Nitrogen was passed for 15 min. through a solution of 0.33 g (1.26 mmol) $RuCl_3{\cdot}3H_2O$ in 37.5 ml of methanol. A solution of 0.51 g (2.58 mmol) tazpy in 12.5 ml of methanol was added. The green mixture was heated to reflux under a nitrogen atmosphere with magnetic stirring for 8 h. After the solution was cooled to room temperature, the residue was isolated by filtration and washed with water and diethyl ether. Recrystallization from chloroform-ether resulted in needle-shaped crystals suitable for X-ray diffraction analysis. The yield was: 0.56 g, 78%. Elemental analysis was calculated for complex **1**, probably containing some residual solvent, $RuC_{24}H_{22}N_6Cl_2{\cdot}1.5H_2O$, C 48.6; H 4.3; N 14.2. The following was found: C 48.9; H 4.5; N 14.8.

α-[Ru(tazpy)$_2$Cl$_2$] (complex **2***)*

To 0.3 g (0.53 mmol) of the crude γ isomer in 45 ml of water and 15 ml of ethanol were added 6 g LiCl and 5.3 ml of 0.01 M NaOH. This mixture was refluxed with stirring for 2 h and then left at room temperature overnight. Black powder was isolated by filtration and washed several times with water and diethyl ether. Recrystallization from chloroform-ether resulted in crystalline material. The yield was: 0.053 g, 18%. Elemental analysis was calculated for $RuC_{24}H_{22}N_6Cl_2$, C 50.9, H 3.9, N 14.8. The following was found: C 50.1, H 3.7, N 14.8.

β-[Ru(tazpy)$_2$Cl$_2$] (complex **3***)*

A suspension of 0.090 g (0.16 mmol) of pure γ-$[Ru(tazpy)_2Cl_2]$ in 9 ml of absolute ethanol and 9 ml of methylene chloride was stirred at room temperature with 0.026 g of NaOH (crushed). The mixture was stirred for ca. 60 h until no γ isomer was present (checked by TLC). The solution was cooled in an ice bath, and 11 drops of concentrated HCl were added. The mixture was evaporated to 9 ml, and 7 ml of diethyl ether was added. The mixture was left overnight, and the precipitate was isolated by filtration and thoroughly washed with water. The yield was: 0.042 g, 38%. Elemental analysis was calculated for $RuC_{24}H_{22}N_6Cl_2$, C 50.9, H 3.9, N 14.8. The following was found: C 50.2, H 4.0, N 13.6.

γ-[Ru(mazpy)$_2$Cl$_2$] (complex **4***)*

The synthesis was carried out analogous to complex **1**. The yield was: 0.95 g, 54%. Elemental analysis was calculated for $RuC_{24}H_{22}N_6Cl_2{\cdot}1.5H_2O$, C 48.6, H 4.3, N 14.2. The following was found: C 48.7, H 4.1, N 14.8.

α-[Ru(mazpy)$_2$Cl$_2$] (complex **5***)*

The synthesis was carried out analogous to complex **2**. The yield was: 0.2 g, 40%.Elemental analysis was calculated for $RuC_{24}H_{22}N_6Cl_2$: C 50.9, H 3.9, N 14.8. The following was found: C 50.4, H 4.05, N 14.7.

β-[Ru(mazpy)$_2$Cl$_2$] (complex **6***)*

Elemental analysis was calculated for $RuC_{24}H_{22}N_6Cl_2$, C 50.9, H 3.9, N 14.8. The following was found: C 50.1, H 4.2, N 14.5. The synthesis was performed analogous to complex **3**, except that the compound was purified over a neutral alumina column. The yield was: 0.050 g, 17%.

Crystallographic studies of complexes **1** and **5**

Single crystals suitable for structure determination were mounted on a Lindemann glass capillary and transferred into the cold nitrogen stream of the diffractometer. Data were collected on a Nonius KappaCCD diffractometer on rotating anode (Mo Kα radiation, graphite monochromator, $\lambda = 0.71073$ Å). Pertinent data for the structure determinations are presented in Table 1. Structures were solved with direct methods using SHELXS86 [19] for structure **1** and SHELXL97 [20] for structure **5**. Refinement

Table 1 Crystallographic data for compounds **1** and **5**

	Compound **1**	Compound **5**
Crystal data		
Formula	$C_{24}H_{22}Cl_2N_6Ru$	$C_{24}H_{22}Cl_2N_6Ru$
Molecular weight	566.45[a]	566.45
Crystal system	Hexagonal	Orthorhombic
Space group	$P6_5$ (no. 170)	*Fdd*2 (no. 43)
a (Å)	22.948(4)	67.664(8)
b (Å)	-	21.676(3)
c (Å)	8.4772(10)	9.8086(12)
V (Å^3)	3,866(11)	14,386(3)
D_{calc} (g/cm^3)	1.460 [a]	1.569
Z	6	24
F ($\times 10^3$)	1,716[a]	6,864
Mo Kα (μm/mm)	0.839[a]	0.901
Crystal colour	Black	Black
Crystal size (mm)	0.05×0.10×0.35	0.05×0.05×0.40
	Data collection	
θ_{min},θ_{max} (°)	0.85, 25.37	1.6, 25.35
Distal crystal detector (mm)	40	50
X-ray exposure (h)	14.8	6.7
Data set	−27:27, −27:27, −10:10	−81:81, −26:26, −7.11
Total data	67,887	33,423
Total unique data	4,724	5,138
R_{int}	0.0856	0.1062
R_σ	0.0347	0.0642
Transmission range	-	0.654–0.956
Refinement		
Refined parameters (no.)	301	450
Flack x[b]	0.01(3)[c]	−0.03(4)
Final *R*1[d]	0.0304 [4411$I > 2\sigma(I)$]	0.0489 [4346$I > 2\sigma(I)$]
Final w *R*2[e]	0.0688	0.1069
Goodness of fit	1.075	1.032
w^{-1}[f]	$\sigma^2(F^2) + (0.0297P)^2 + 2.39P$	$\sigma^2(F^2) + (0.0583P)^2 + 16.23P$
Minimum and maximum residual density (e/Å^3)	−0.28, 0.35	−0.68, 0.95

[a]Excluding disordered solvent contribution
[b]See Reference [42]
[c]Determined in a racemic twin refinement
[d]$R1 = \Sigma||Fo|-|Fc||/\Sigma|Fo|$
[e]w $R2 = [\Sigma[w(F_o^2-F_c^2)^2]/\Sigma[w(F_o^2)^2]]^{1/2}$
[f]$P = Max(F_o^2,0) + 2F_c^2/3$

on F^2 was performed with SHELXL-97 [21]. The hydrogen atoms were included in the refinement on calculated positions riding on their carrier atoms. The methyl moieties were refined as a rigid group, allowing for rotation along the C–C bond. The non-hydrogen atoms were refined with anisotropic displacement parameters. The hydrogen atoms were refined with a fixed isotropic displacement parameter related to the value of the equivalent isotropic displacement parameter of their carrier atoms.

In structure **1**, a channel of disordered solvent molecules was found, located on the 6_5 screw axis. No satisfactory disorder model could be found. The associated contribution to the structure factors was taken into account using the SQUEEZE procedure [22] as incorporated in PLATON [23]. A total amount of 74 *e* was found in a volume of 429 Å^3 per unit cell.

For complex **5**, an empirical absorption correction was performed, based on the intensity differences found for multiple measurements of symmetry-related reflections (MULABS) [23].

Neutral atom-scattering factors and anomalous dispersion corrections were taken from the International Tables for Crystallography [24]. Geometrical calculations and illustrations were performed with PLATON [23]; all calculations were performed on a DEC Alpha 255 station.

Crystallographic data (without structure factors) for the structures reported in this paper were deposited with the Cambridge Crystallographic Data Centre as supplementary publication no CCDC-223969 and CCDC-223970. Copies of the data can be obtained free of charge from the CCDC (12 Union Road, Cambridge CB2 1EZ, UK; Tel.: +44-1223-336408; Fax: +44-1223-336033; e-mail: deposit@chemcrys.cam.ac.uk; http://www.ccdc.cam.ac.uk).

Physical measurements

The NMR experiments were performed at 300.13 MHz on a Bruker 300 DPX spectrometer and at 600.13 MHz on a 600 DPX. Spectra were recorded in $CDCl_3$. All spectra were obtained at 25 °C unless otherwise noted. 2D ^{1}H–^{1}H NOESY spectra were performed with a mixing time of 1 s, eight scans per t_1 increment and a relaxation delay of 1 s. Elemental analysis (C, H and N) was carried out on a Perkin Elmer 2400 CHNS analyzer by the Gorlaeus Laboratories of Leiden University.

Cytotoxicity tests

RPMI and FCS were obtained from Life Technologies (Paisley, UK). SRB, DMSO, penicillin and streptomycin were obtained from Sigma (St. Louis, MO, USA), TCA and acetic acid from Baker BV (Deventer, NL) and PBS from NPBI BV (Emmer Compascuum, NL).

The test and reference compounds were dissolved to a concentration of 0.25 mg/ml in full medium, by 20-fold dilution of a stock solution containing 1 mg compound/200 μl DMSO. For the determination of the IC_{50} values, the following panel of human tumour cell lines was used: MCF-7 (breast cancer), EVSA-T (breast cancer), WIDR (colon cancer), IGROV (ovarian cancer), M19 (melanoma), A498 (renal cancer) and H226 (non-small cell lung cancer).We used these cell lines as obtained directly from the NCI (USA); they are well characterized [25], and their responsiveness to a range of standard cytostatics is known. Cytotoxicity was estimated by the microculture sulforhodamine B (SRB) test [26].

5-Day cell exposure

On day 0, 1.5×10^3 cells in 150 µl complete medium, harvested by trypsin treatment from donor cultures, were plated in 96-well flat-bottom microtiter plates (Falcon 3072, BD). Plates were preincubated for 48 h at 37 ºC, 8.5% CO_2, to facilitate the cells to adhere.

On day 2, a three-fold dilution sequence of ten steps was made in full medium, starting with the 0.25 mg/ml solution. Every dilution was used in quadruplicate by adding 50 µl to a column of four wells. On day 7, the incubation was terminated by washing the plate twice with PBS. Subsequently cells were fixed with 10% trichloroacetic acid in PBS and placed at 4 °C for 1 h. After five washings with tap water, cells were stained for at least 15 min with 0.4% SRB dissolved in 1% acetic acid. After staining, cells were washed with 1% acetic acid to 150 µl 10 mM tris-base. The absorbance was read at 540 nm using an automatic microplate reader (Labsystems Multiskan MS). Data were used for construction of concentration response curves and determination of the IC_{50} value by use of Deltasoft 3 software.

1-h Cell exposure

In this experiment, TS/A murine adenocarcinoma cells were used. The IC_{50} values of α-, β- and γ-$[Ru(azpy)_2Cl_2]$ in this cell line (0.12, 3.0 and 0.44 µM, respectively) are analogous to the values in the panel of cell lines (Table 5). TS/A cells (10^4 per well) were seeded in 100 µl complete medium in 96-multiwell flat-bottom microtiter plates (Corning Costar). The plates were preincubated for 48 h to allow cell adhesion. A stock solution of all compounds (1 mM in DMSO) was freshly prepared, and the test concentration of 0.01 mM was obtained by a 1:100 dilution in PBS^{CaMg}. PBS^{CaMg} is phosphate-buffered saline containing 0.9 mM $CaCl_2{\cdot}2H_2O$ and 0.5 mM $MgCl_2{\cdot}6H_2O$. PBS^{CaMg} is used instead of normal PBS to facilitate adherence of the cells. 100 µl of this solution containing the test compound was added to the wells, from which the complete medium was previously removed. The control group consisted of PBS^{CaMg} with 1% DMSO (which corresponds to the percentage of DMSO in each tested solution). The plates were incubated for 1 h at 37 °C, 5% CO_2. At the end of the incubation time, cells were washed twice with PBS and allowed to grow for an additional 24 h in 100 µl complete medium, and the evaluation of cell proliferation was performed by the MTT colorimetric assay [27], as described below.

Atomic absorption spectroscopy has been used to measure the amount of ruthenium inside the cells (see below). 0.7×10^6 cells/well were seeded in triplicate in six-well plates (Corning Costar), and allowed to grow for 48 h before treatment with 0.01 mM ruthenium solutions. As for the MTT test, the solutions were washed away after 1 h of treatment in PBS^{CaMg}. The cells were collected by trypsination, and after three washing steps were submitted to flameless atomic absorption spectroscopy detection of the cell content of ruthenium.

Atomic absorption spectroscopy

The intracellular ruthenium content in treated cells was determined by atomic absorption spectroscopy. Samples were processed according to a modification of the procedures described by Tamura et al. [28]. All specimens were dried in cryo-vials. A first step of desiccation was performed overnight at 80 °C, a second step at 105 °C, until the samples reached the constant exsiccated weight. The lysis of the desiccated samples was carried out with the addition of 100 µl of tetramethylammonium hydroxide (TMAH) at 25% in water (Aldrich Chimica, Italy) and 100 µl of milliQ directly in the vials. Volumes were adjusted to 0.5 ml with milliQ water.

Ruthenium quantitation: the concentration of ruthenium in biological samples was measured in triplicate by means of graphite furnace atomic absorption spectrometry (GFAAS), model SpectrAA-300, supplied with a specific ruthenium emission lamp (hollow cathode lamp P/N 56–101447–00, Varian, Mulgrave, Vic., Australia). Before each daily analysis session, a five-point calibration curve was traced using Ruthenium Custom-Grade Standard 998 mg/ml (Inorganic Ventures, St. Louis, USA).

In order to correct for possible deterioration of the graphite furnace during a daily working session, the calibration curve was re-traced after every 12 samples, and a standard was measured every six samples. The lower and higher limits of quantitation (LLQ, HLQ) were set at the concentration levels that correspond to the lowest and highest standard concentrations employed, respectively. The limit of detection (LOD) was estimated according to the EURACHEM guide. LLQ, HLQ and LOD were 20, 100 and ~10 ng Ru/ml of sample, respectively. The quantitation of ruthenium was carried out in 10-µl samples at 349.9 nm with an atomising temperature of 2,500 °C, using argon as purge gas at a flow rate of 3.0 l/min. Further details concerning the furnace parameter settings are described in the literature [29].

MTT colorimetric assay

The MTT assay [27] is based on the mitochondrial reduction of the tetrazolium salt MTT (3-(4,5-dimethylthiazol-2-yl)-2,5-diphenyl-2H-tetrazolium bromide) by actively growing cells to produce blue insoluble purple formazan crystals. A 50-µl MTT solution (5 mg/ml in PBS, Sigma Chemical Co.) was added to each well and incubated for 2–4 h. After removing the surnatant, the formed formazan crystals were dissolved in 100 µl DMSO. Optical density (OD) was measured by the microplate reader at 590 nm. The absorbance is directly proportional to cell viability.

Statistical analysis

Data were submitted to computer-assisted statistical analysis using the Student t-test for grouped data. Data were considered to be statistically significant if the probability factor, p, was <0.05, <0.01 and <0.001. Symbols used to identify the significance are $*p<0.05$, $**p<0.01$ and $***p<0.001$.

Results and discussion

General considerations

Although only the three main α, β and γ isomers of $[Ru(tazpy)_2Cl_2]$ and $[Ru(mazpy)_2Cl_2]$ are considered, a few remarks will be made concerning the δ and ϵ isomers. The ϵ isomer (with coordinating pairs of Cl ligands *cis*, Npy atoms *cis* and Nazo nitrogen atoms *trans*) is not formed under normal conditions [12], and moreover, as it will isomerize to another isomer under physiological temperatures, it is not suitable for a study of structural and biological properties. The δ isomer of $[Ru(azpy)_2Cl_2]$ (δ indicates the coordinating pairs Cl, Npy and Nazo *trans*, *trans*, *trans*) is formed as a side product in the synthesis of γ-$[Ru(azpy)_2Cl_2]$, and it has recently been fully characterized [11]. The γ isomer of $[Ru(azpy)_2Cl_2]$ has been shown to be kinetically the most favoured isomer, and it is found as the main product in the synthesis of the crude mixture of isomers starting from $RuCl_3{\cdot}xH_2O$ in methanol [9], as well as from *cis*-$[Ru(dmso)_4Cl_2]$ in acetone [10].

In both syntheses, the presence of small amounts of δ isomer has been reported, in 5% and 20% yield, respectively [11]. Interestingly, the δ isomer has not been

detected by NMR in the crude product obtained after the synthesis of γ-[Ru(mazpy)$_2$Cl$_2$] from RuCl$_3$ and mazpy in methanol. As the methyl group of the mazpy ligand is positioned opposite the pyridine nitrogen, it is not imposing any steric hindrance towards the other azpy ligand in the δ configuration. On the other hand, the reason for the absence of δ formation might also be caused by solubility differences. NMR data of the crude product of the γ-[Ru(tazpy)$_2$Cl$_2$] show a small amount of "impurity", more likely a ligand impurity, although it was impossible to assign the signals owing to overlapping resonances.

The X-ray structure determination of the γ isomeric complexes shows the presence of solvent molecules in the channels (see below), and correspondingly in the calculated elemental analyses of the γ isomers some H_2O has been added to compensate for lattice impurities. In the solid-state structure, the molecules are stacked in helices along the six-fold screw axis (see below). A solvent-filled channel with a radius of ca. 4 Å is in the centre of each helix. From calculations, it has been determined that approximately 1.3–2.3 water molecules are present for each ruthenium, consistent with the elemental analysis data.

The column purification in the case of complex **6** and not recovering the filtrate in the case of crystallization of complex **2** are the reasons for some low yields.

X-Ray structural characterization of γ-[Ru(tazpy)$_2$Cl$_2$]

The molecular structure of γ-[Ru(tazpy)$_2$Cl$_2$], complex **1**, is shown in Fig. 3. Crystallographic data for complex **1** are listed in Table 1. Selected bond distances (Å) and angles (°) for complex **1** are listed in Table 2.

As the coordinating pairs Cl, N(py), and N(azo) are positioned *trans*, *cis*, *cis* (tcc) the configuration is called the γ isomer [8,30]. Although the γ-[Ru(azpy)$_2$Cl$_2$] complex was erroneously characterized in early literature, nowadays several X-ray structure determinations of γ isomeric complexes of the type [RuL$_2$Cl$_2$] (with L, an asymmetric azo-containing didentate ligand) are known [8, 31, 32, 33, 34]. Distances and angles of complex **1** are

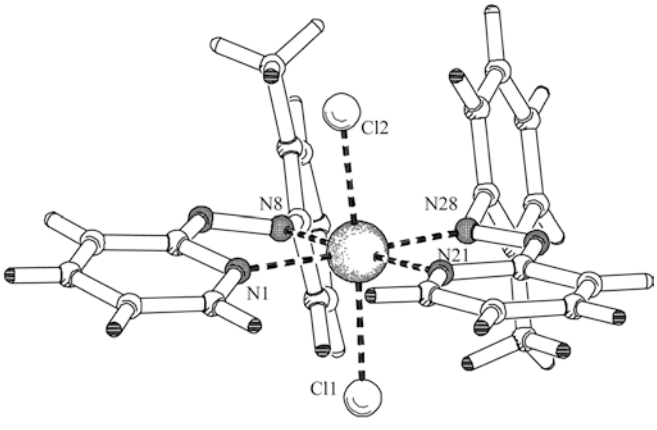

Fig. 3 Molecular structure of γ-[Ru(tazpy)$_2$Cl$_2$]

Table 2 Selected bond distances (Å) and angles (°) of compound **1**

Ru(1)–Cl(1)	2.3843(11)	Cl(1)–Ru(1)–N(21)	84.71(9)
Ru(1)–Cl(2)	2.3665(12)	Cl(1)–Ru(1)–N(28)	90.94(9)
Ru(1)–N(1)	2.085(3)	Cl(2)–Ru(1)–N(1)	85.82(10)
Ru(1)–N(8)	1.961(4)	Cl(2)–Ru(1)–N(8)	94.45(10)
Ru(1)–N(21)	2.103(3)	Cl(2)–Ru(1)–N(21)	86.85(9)
Ru(1)–N(28)	1.975(3)	Cl(2)–Ru(1)–N(28)	95.50(9)
N(7)–N(8)	1.300(4)	N(1)–Ru(1)–N(8)	76.12(13)
N(27)–N(28)	1.294(4)	N(1)–Ru(1)–N(21)	105.65(12)
		N(1)–Ru(1)–N(28)	178.01(14)
Cl(1)–Ru(1)–Cl(2)	167.83(4)	N(8)–Ru(1)–N(21)	177.89(13)
Cl(1)–Ru(1)–N(1)	88.02(9)	N(8)–Ru(1)–N(28)	102.28(13)
Cl(1)–Ru(1)–N(8)	94.25(10)	N(21)–Ru(1)–N(28)	75.93(12)

comparable to the related structure γ-[Ru(azpy)$_2$Cl$_2$] [8, 30]. An extensive description of the crystal structure of γ-[Ru(azpy)$_2$Cl$_2$] has been reported recently [8, 30]. The crystals of complex **1** have the relatively rare hexagonal space group $P6_5$, which is the same as for γ-[Ru(azpy)$_2$Cl$_2$]. The molecular structure of complex **1** contains channels located on a six-fold screw axis in which strongly disordered solvent is present. Interestingly, the X-ray structure of complex **1** shows the close proximity of the phenyl rings and the position of the methyl groups, which are positioned antiparallel to provide enough space for these relatively large substituents.

The geometric centres of the two phenyl rings are 3.496(3) Å apart intramolecularly, and the angle between the ring planes is 13.1(2) °. These values are comparable to those of the same parameters in the structure of γ-[Ru(azpy)$_2$Cl$_2$]; 3.493(8) Å and 16.9(2)°. In the related structure γ-[Ru(papm)$_2$Cl$_2$] (papm = 2-phenylazopyrimidine) [31], the planar phenyl rings are also close to each other (3.716 Å). Besides the stacking between the phenyl rings of one molecule of complex **1**, the pyridine rings of the molecules (x,y,z) and (x,y,z + 1) also display π–π stacking, since the geometric centres of the two pyridine rings are 4.079(3) Å apart, and the angle between the rings is 9.9(2)°.

The phenyl rings of complex **1** are almost perpendicular with respect to the pyridine plane, which is different in comparison to the analogous compound γ-[Ru(azpy)$_2$Cl$_2$] (Fig. 4). The angles between the pyridine ring and phenyl ring of complex **1** are 76.1(2)° and 73.0(2)°, which is quite different from the corresponding angles in γ-[Ru(azpy)$_2$Cl$_2$], i.e. 54.2(4)° and 52.7(3)°. In the compound γ-[Ru(papm)$_2$Cl$_2$], the phenyl rings are inclined at angles of 41° and 35° relative to the chelated azo pyrimidine plane. A space-filling model of complex **1** (Fig. 4) shows that in the almost perpendicular orientation of the phenyl rings, the methyl groups do not show steric hindrance. The origin of the more perpendicular orientation of the phenyl rings in complex **1** related to γ-[Ru(azpy)$_2$Cl$_2$] is not clear.

X-Ray structural characterization of α-[Ru(mazpy)$_2$Cl$_2$]

A projection of the X-ray structure of α-[Ru(mazpy)$_2$Cl$_2$], complex **5**, is shown in Fig. 5. For clarity, only

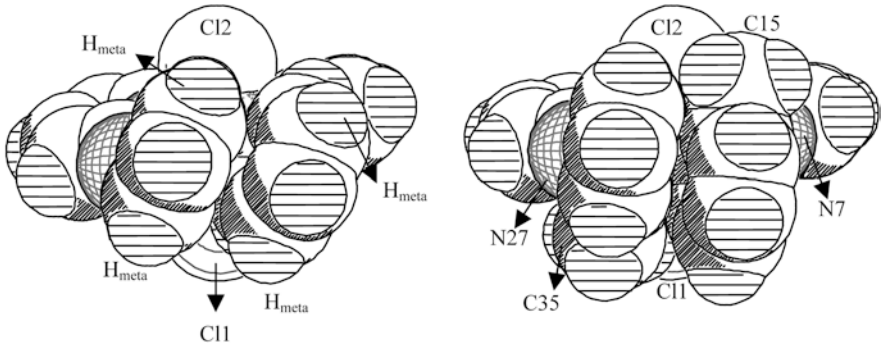

Fig. 4 Space-filling plots of the solid-state structures of γ-$[Ru(azpy)_2Cl_2]$[8] (*left*) and complex **1** (*right*) showing the different orientations of the phenyl rings related to the pyridine ring planes

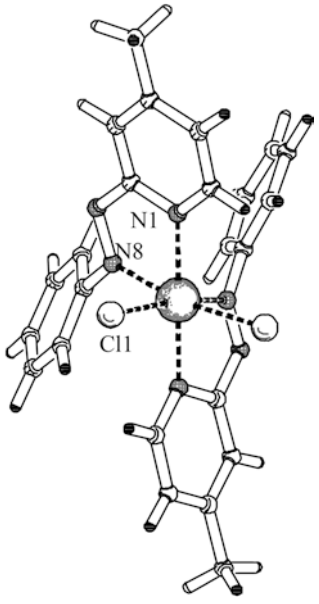

Fig. 5 Molecular structure of the Δ enantiomer of α-$[Ru(mazpy)_2Cl_2]$

the Δ isomer is shown, while the unit cell of course does contain one of each enantiomer. Crystallographic data of complex **5** are included in Table 1. Selected bond distances (Å) and angles (°) for complex **5** are listed in Table 3. The asymmetric unit contains one complete Ru-complex at a general position and a Ru-complex located at a two-fold rotation axis, half of which is unique. If the coordinating pairs Cl, N(py), and N(azo) are considered in that order, the configuration of complex **5** is *cis*, *trans*, *cis* (ctc), the so-called α configuration. The Ru–N(py), Ru–N(azo) and Ru–Cl distances are almost identical to those in the related structure α-$[Ru(azpy)_2Cl_2]$ [35]. The angle Cl–Ru–Cl in complex **5** (94.4°) is slightly bigger than in α-$[Ru(azpy)_2Cl_2]$ (89.4°). No stacking interactions have been observed in the lattice.

NMR characterization of complexes **1–6**

In a recent publication, the use of 2D NOESY NMR spectroscopy was proven to be useful in determining the isomeric structure of the isomers of $[Ru(azpy)_2Cl_2]$ complexes [11]. The complexes α- and γ-$[Ru(azpy)_2Cl_2]$ have a C_2 symmetry, causing the two azpy ligands in each isomer to be identical in NMR. It was proven that the α configuration shows a characteristic (intramolecular) interligand H6–H(o) (H(o) = H10/H14) NOE cross-peak [11, 36, 37].[1] Moreover, the averaged interproton H6–H(o) distances from solid-state XRD-data appear to be useful for predicting NOEs in solution [11, 36, 37]. The absence of interligand NOE cross-peaks between the aromatic resonances is characteristic for the γ isomer [11].

Table 3 Selected bond distances (Å) and angles (°) of complex **5**. Suffix a denotes symmetry operation 1/2-*x*, 1/2-*y*,*z*

Ru(1)–Cl(1)	2.392(2)	Cl(1)–Ru(1)–N(8)a	169.92(14)
Ru(1)–N(1)	2.041(4)	N(1)–Ru(1)–N(8)	76.0(2)
Ru(1)–N(8)	1.977(6)	N(1)–Ru(1)–N(8)a	105.0(2)
N(7)–N(8)	1.300(6)	N(8)–Ru(1)–N(8)a	88.4(2)
Ru(2)–Cl(21)	2.395(2)	Cl(21)–Ru(2)–Cl(22)	93.74(7)
Ru(2)–Cl(22)	2.383(2)	Cl(21)–Ru(2)–N(21)	94.59(16)
Ru(2)–N(21)	2.045(4)	Cl(21)–Ru(2)–N(28)	168.51(15)
Ru(2)–N(28)	1.967(5)	Cl(21)–Ru(2)–N(41)	82.12(17)
Ru(2)–N(41)	2.054(4)	Cl(21)–Ru(2)–N(48)	87.56(16)
Ru(2)–N(48)	1.967(5)	Cl(22)–Ru(2)–N(21)	82.03(18)
N(27)–N(28)	1.296(6)	Cl(22)–Ru(2)–N(28)	92.05(16)
N(47)–N(48)	1.308	Cl(22)–Ru(2)–N(41)	93.31(18)
		Cl(22)–Ru(2)–N(48)	169.73(14)
		N(21)–Ru(2)–N(28)	76.4(2)
Cl(1)–Ru(1)–N(1)	84.00(18)	N(21)–Ru(2)–N(41)	174.1(3)
Cl(1)–Ru(1)–N(8)	89.41(17)	N(21)–Ru(2)–N(48)	108.0(2)
Cl(1)–Ru(1)–N(8)	89.41(17)	N(28)–Ru(2)–N(41)	107.5(2)
Cl(1)–Ru(1)–Cl(1)a	94.40(7)	N(28)–Ru(2)–N(48)	88.5(2)
Cl(1)–Ru(1)–N(1)a	95.11(18)	N(41)–Ru(2)–N(48)	76.8(2)

[1] In the C_2, symmetric γ and α isomers of the $[Ru(azpy)_2Cl_2]$ complexes, the two azpy ligands are equivalent. Therefore, it is not clear beforehand whether an NOE is an (intramolecular) inter- or intraligand NOE cross-peak. However, the NOE H6–H(o) in the α isomer of α-$[Ru(azpy)_2Cl_2]$ is definitely an interligand one, for example. Obviously from the distance H6–H(o) within one azpy ligand of α-$[Ru(azpy)_2Cl_2]$, as derived from the X-ray structure [35] (on average 6.31 Å), it is clear that no intraligand NOE can be expected. The interligand H6–H(o) distance, as shown in the X-ray structure, is on average 4.14 Å, predicting the interligand NOE. Moreover, in asymmetric α-isomeric azpy complexes [37], like α-$[Ru(azpy)_2(9\text{-Egua})(H_2O)](PF_6)_2$ or α-$[Ru(azpy)_2Cl(NO_3)]$ (unpublished data), the interligand H6–o' and H6'–o (prime denoting the other azpy ligand) are observed and not, for example, the intraligand H6–o NOE.

The ^{1}H NMR spectrum of complex **1** shows a symmetric complex, and the assignment of the signals and determination of the configuration has been performed using 2D COSY and 2D NOESY NMR. The chemical shift values are mentioned in Table 4. The aromatic region of the 2D NOESY NMR spectrum does not show any NOE signals, as expected for the γ isomer [11]. Nevertheless, the CH_3 resonance shows both intra- and interligand NOE signals, which are used to complete the assignment (see Fig. S1 in Electronic Supplementary Material). The assignment of the H11 and H14 atoms has been done using deshielding arguments caused by the deshielding effect [38] of the Cl ligands. In general, in ruthenium azpy complexes, [Ru(azpy)$_2$Cl$_2$], particularly the H6 and H(o) protons, are characteristically shifted due to the shielding and deshielding effect of neighbouring ligands in the distinct isomers [11]. The H14 atom is, according to the X-ray structure, closer to one Cl ligand than the H11 atom, and even though in solution synchronous flipping of the phenyl rings is proposed (see below), the H14 is still closest to one Cl ligand. Therefore, it is reasonable to assume that the resonance at low field corresponds to H14, and the resonance at high field to the H11 atom.

An important difference between the ^{1}H NMR spectrum of complex **1** and the complex γ-[Ru(azpy)$_2$Cl$_2$] is the fact that in complex **1** four inequivalent phenyl-ring hydrogen atoms are present, so four resonances appear instead of three, i.e. *o*, *m* and *p* for γ-[Ru(azpy)$_2$Cl$_2$]. Synchronous flipping of the phenyl rings at about 90º is proposed in γ-[Ru(azpy)$_2$Cl$_2$] (fast on the NMR time scale, even at low temperatures) to account for the appearance of only one *ortho* and *meta* resonance [8, 11]. In the case of complex **1**, cooling of the sample results in a second set of signals, besides one set of main signals. The second set of resonances are only slightly shifted with respect to the main signals and have a very small intensity ($< 5\%$) at low temperatures. Owing to the low intensity of the second set of signals, it was impossible to determine the orientation of the phenyl rings in this atropisomer. Speculatively, in solution at room temperature, the phenyl rings of complex **1** are also involved in a synchronous flipping of the phenyl rings by 90° (45° back and forth about the almost perpendicular solid-state orientation). At low temperatures, two orientations are likely, of which the most abundant atropisomer probably corresponds to the solid-state structure.

The chemical shift values of complex **2** are listed in Table 4. Again, one set of signals is present, due to the fact that the complex is C_2-symmetric. The assignment of all resonances was done by the use of 2D COSY and NOESY NMR spectroscopy. The 2D NOESY NMR data show as most important cross-peaks: an interligand NOE between the H6 resonance and H14 resonance, and an interligand NOE between the H6 and CH_3 resonance. As it is known that in case of the α-Ru(azpy)$_2$ backbone, an H6–H(o) interligand NOE cross-peak is to be expected [11, 36, 37], these H6–H14 and H6–CH_3 NOEs confirm the α configuration. The fact that the H6 resonance gives an NOE to both the CH_3 signal, as well as to the H14 resonance, suggests the fast rotation of the phenyl rings in solution, a common feature of α isomeric complexes, despite the presence of the methyl groups.

The aromatic region of the ^{1}H NMR spectrum of complex **3** shows a double set of sharp azpy signals at room temperature. The two azpy ligands are no longer equivalent due to the absence of a C_2 axis. Based on the fact that the two azpy ligands are not equivalent, one should also expect two methyl signals. However, only one broad signal is present at 1.67 ppm. It is likely that the other methyl signal is too broad to be detected. Cooling down the sample in the NMR tube results in a difficult pattern of broad and sharp signals in the aromatic region and high-field region. The complete investigation of the rotational aspects of the phenyl rings has not been attempted. Table 4 includes the chemical shift values of the resonances of complex **3**. However, due to the fact that one of the methyl groups cannot be detected at room temperature, it was impossible to distinguish which phenyl-ring signals belong to which pyridine-ring signals.

The NMR characterization of the isomeric [Ru(mazpy)$_2$Cl$_2$] complexes is reasonably straightforward and is relatively more easily done than for the corresponding tazpy complexes. The methyl group on the pyridine ring facilitates the NMR spectra. The chemical shift values of the ^{1}H NMR resonances of

Table 4 ^{1}H NMR Chemical shift values of complexes **1–6** in $CDCl_3$

	H6/H6′	H5/H5′	H4/H4′	H3/H3′	H11/H11′	H12/H12′	H13/H13′	H14/H14′	CH_3/CH_3'
1	8.94	7.85	8.19	8.54	6.83	7.00	6.86	7.40	2.14
2	9.17	7.40	7.96	8.54	7.18	7.09	6.65	5.86	2.40
3[a]	9.69	7.77	7.95	8.40	[b]	[b]	[b]	[b]	[b]
	7.12	7.02	7.75	8.28					
					o/o′	m/m′	p/p′		
4	8.78	7.64	-	8.44	7.57	7.00	7.20	-	2.79
5	9.19	7.32	-	8.32	6.85	7.11	7.26	-	2.65
6	9.59	7.67	-	8.33	6.71	7.19	7.37	-	2.78
	7.08	7.08		8.23	7.79	7.35	7.39	-	2.59

[a]Spectrum recorded at 600 MHz
[b]The phenyl ring signals of **3** remain unresolved as one CH_3 signal was broadened, and the other was too broad to be detected

complexes **4–6** are listed in Table 4 and do not require detailed discussion.

Cytotoxicity

In the cytotoxicity tests, the *cis*-isomers (α and β) have been tested as racemic mixture.

A DMSO stock solution was used in the cytotoxicity tests of the [Ru(azpy)$_2$Cl$_2$] complexes, as these complexes are poorly water soluble. NMR data, mass spectrometry and conductivity measurements of α-[Ru(azpy)$_2$Cl$_2$] in an aqueous solution containing DMSO excludes the possibility that DMSO may coordinate in place of the chloride ligands [36].

The cytotoxicity data of the parent complexes α, β, and γ-[Ru(azpy)$_2$Cl$_2$] and the complexes **1–6** compared with cisplatin and 5-fluorouracil, in a series of human tumour cell lines, are listed in Table 5. As reported earlier [8], the complex α-[Ru(azpy)$_2$Cl$_2$] shows a very pronounced cytotoxicity, higher than that of cisplatin in all cell lines. The β-[Ru(azpy)$_2$Cl$_2$] is approximately a factor of 10 less active than the α isomer and, in contrast to literature data [8], γ-[Ru(azpy)$_2$Cl$_2$] shows an activity comparable to that of the α isomer.

To exclude any effect due to the presence of impurities in the test samples, several batches have been investigated, and great care was taken in dissolving the compounds in order to avoid excessive heating of the samples; it is known that above 40 °C, isomerization can occur [37]. The reason for the reported inactivity of the γ-isomer [8] might be that the sample was excessively heated to let it dissolve, and it is likely that the species tested has been the far less active β-isomer. Another reason for the earlier reported inactivity of γ-[Ru(azpy)$_2$Cl$_2$] might be due to solubility problems. The γ-isomer is the least soluble isomer, so it might have been precipitated, resulting in a much lower concentration than if it had been in contact with the cells.

In comparison to the parent complexes α, β and γ-[Ru(azpy)$_2$Cl$_2$], the compound α-[Ru(tazpy)$_2$Cl$_2$] is more active in all cell lines, except on A498 renal cancer cells. β-[Ru(tazpy)$_2$Cl$_2$] is less active in all cell lines, and the activity of γ-[Ru(tazpy)$_2$Cl$_2$] is not different from the parent complex.

The complexes α and β-[Ru(mazpy)$_2$Cl$_2$] are slightly less active than the analogous isomeric azpy complexes in most cell lines, and γ-[Ru(mazpy)$_2$Cl$_2$] does not differ from γ-[Ru(azpy)$_2$Cl$_2$].

Apart from these small differences of cytotoxicity caused by a methyl group on the ligands, the main trend of the isomers remains clear: the α isomer of the [RuL$_2$Cl$_2$] complexes (L = azpy, tazpy or mazpy) displays a very high cytotoxicity, whereas the β isomer is approximately a factor of 10 less active. The γ isomer of the [RuL$_2$Cl$_2$] complexes shows in all cases a very high activity, in the same range as the α isomer with the respective ligand.

Potential origins for cytotoxicity differences

The reasons behind the differences in cytotoxicity of the isomeric [RuL$_2$Cl$_2$] complexes are far from being understood. At this stage, it is reasonable to think that these differences might originate from a different interaction of the isomers with their biological target, i.e. DNA [30]. With regard to the *cis*-dichlorobis(azpy)ruthenium(II) complexes, it has been suggested that the differences between the α and β-[Ru(azpy)$_2$Cl$_2$] isomers might depend on the accessibility to DNA coordination [11]. While the monofunctional binding of guanine derivatives is very similar for the two isomers [37, 39], the bifunctional coordination of the purine model base 1-methylbenzimidazole to the α-isomer is sterically less hindered than for the β-isomer [40, 41].

In addition, differences of uptake and transport into cells might vary among the isomers. To study the influence of cellular uptake on the antiproliferative activity, TS/A murine adenocarcinoma cells were treated for 1 h with the α-, β- and γ-[Ru(azpy)$_2$Cl$_2$] complexes at a relatively high concentration (0.01 mM). The amount of ruthenium was determined by flameless atomic absorption spectroscopy, and the effect on cell growth was studied by MTT colorimetric assay. The amount of ruthenium inside the treated cells after 1 h of treatment

Table 5 IC_{50} values (μM) of a series of ruthenium(II) complexes, cisplatin and 5-fluorouracil against a series of tumor-cell lines (MCF-7, EVSA-T, WIDR, IGROV, M19, A498 and H266)

Tested compound	A498	EVSA-T	H226	IGROV	M19	MCF-7	WIDR
α-[Ru(azpy)$_2$Cl$_2$]	0.27	0.063	0.48	0.27	0.064	0.27	0.27
β-[Ru(azpy)$_2$Cl$_2$]	8.8	0.96	13	3.4	0.75	6.2	11
γ-[Ru(azpy)$_2$Cl$_2$]	0.20	0.019	0.17	0.041	0.017	0.052	0.065
α-[Ru(tazpy)$_2$Cl$_2$]	0.36	<0.0056	0.030	0.0088	<0.006	0.021	0.045
β-[Ru(tazpy)$_2$Cl$_2$]	74	17	29	30	15	32	52
γ-[Ru(tazpy)$_2$Cl$_2$]	1.2	0.011	0.083	0.077	0.019	0.093	0.23
α-[Ru(mazpy)$_2$Cl$_2$]	1.1	0.079	0.46	0.22	0.065	0.42	0.80
β-[Ru(mazpy)$_2$Cl$_2$]	43	2.5	18	14	4.8	15	21
γ-[Ru(mazpy)$_2$Cl$_2$]	0.50	0.013	0.17	0.14	<0.006	0.079	0.20
Cisplatin	7.5	1.4	11	0.6	1.9	2.3	3.2
5-Fluorouracil	1.1	3.7	2.6	2.3	3.4	5.8	1.7

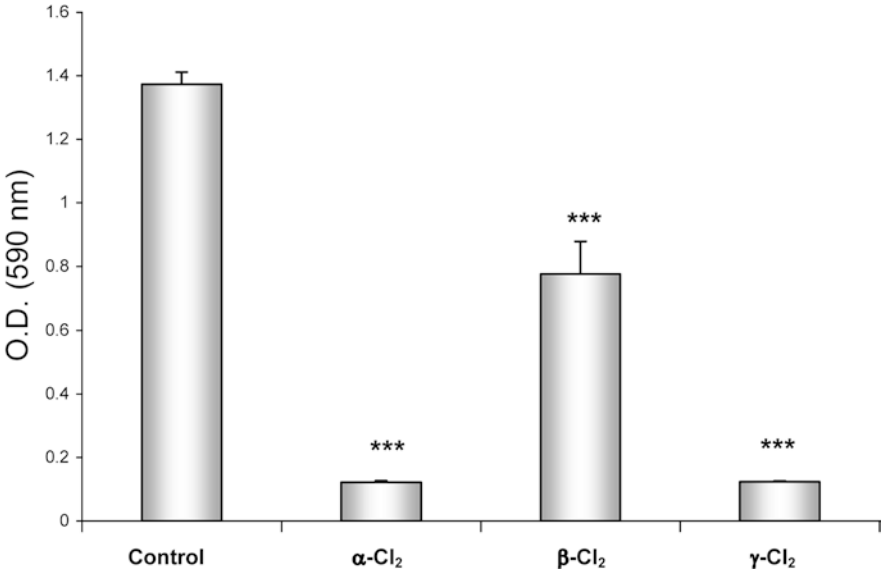

Fig. 6 Reduction of cell proliferation in the TS/A cell line, 24 h after 1 h of drug exposure to the compounds α-$[Ru(azpy)_2Cl_2]$ (α-Cl_2), β-$[Ru(azpy)_2Cl_2]$ (β-Cl_2) and γ-$[Ru(azpy)_2Cl_2]$ (γ-Cl_2) at 0.01 mM. Statistical analysis, Student's t-test , $***p < 0.001$ vs. control

is six-fold higher for the α isomer (0.0160 μg in 1×10^6 cells) than for the β isomer (0.0028 μg in 1×10^6 cells).

Unfortunately, the ruthenium uptake of the γ isomer could not be determined correctly, since it precipitates during treatment and cannot be removed from the cell pellet after washing, leading to incorrect AAS values. The reduction of TS/A cell proliferation (Fig. 6) under these conditions is appreciable with α-$[Ru(azpy)_2Cl_2]$ and γ-$[Ru(azpy)_2Cl_2]$ (reduction to 10% of controls), and is much less evident with β-$[Ru(azpy)_2Cl_2]$ (reduction to 50% of controls), although in both cases the difference is statistically significant. These data suggest that the reduction of cell proliferation after 1 h of treatment is related to cell uptake of the test compounds, although we cannot exclude the possibility that differences in the velocity of DNA interaction may also play a role.

In general, the cytotoxicity of this class of complexes is very promising, but more in vitro and in vivo experiments are needed for a better understanding of the mechanisms underlying their antitumour activity.

Conclusions

The series of novel $[Ru(mazpy)_2Cl_2]$ and $[Ru(tazpy)_2Cl_2]$ (mazpy = 4-methyl-2-phenylazopyridine and tazpy = *o*-tolylazopyridine) have been synthesized and chemically characterized. Small differences in structural aspects due to the additional methyl group on the azpy ligand are best demonstrated in case of γ-$[Ru(tazpy)_2Cl_2]$ compared with γ-$[Ru(azpy)_2Cl_2]$, as shown by X-ray structure determination and NMR spectroscopy in solution.

The series of isomeric $[RuL_2Cl_2]$ complexes (with L = 2-phenylazopyridine, 4-methyl-2-phenylazopyridine or *o*-tolylazopyridine) display a very promising cytotoxic activity in the panel of cell lines MCF-7, EVSA-T, WIDR, IGROV, M19, A498 and H266. Small differences in activity due to the additional methyl group are, for example, shown in the case of α-$[Ru(tazpy)_2Cl_2]$, which is more active than α-$[Ru(azpy)_2Cl_2]$ in almost all cell lines. Most importantly, the cytotoxicity data of the series of methylated-azpy ruthenium(II) complexes establish and confirm the general trend of activities of the isomeric ruthenium(II) (methyl)azpy complexes: the α isomer is highly cytotoxic, the β isomer is a factor of 10 less cytotoxic, and the γ isomer also displays a very high cytotoxicity. So, interestingly, the three isomers of the (methylated) azpy ruthenium(II) complexes show that, although they are structurally related, there is a pronounced difference in their pattern of cytotoxic activity.

Acknowledgements This work was supported by the Council for Chemical Sciences of the Netherlands Organisation for Scientific Research (CW-NWO). We thank Johnson Matthey Chemicals (Reading, UK) for a generous loan of $RuCl_3{\cdot}3H_2O$. Additional support from COST Action D20, allowing regular research exchanges to partner laboratories inside EU countries, is gratefully acknowledged. Marina Bacac is grateful to the Callerio Foundation for providing a three-year fellowship grant.

References

1. Clarke MJ, Zhu FC, Frasca DR (1999) Chem Rev 99:2511–2533
2. Clarke MJ (2002) Coord Chem Rev 232:69–93
3. Reedijk J (2003) Proc Natl Acad Sci USA 100:3611–3616
4. Lippert B (ed) (1999) Cisplatin. chemistry and biochemistry of a leading anticancer drug. Verlag Helvetica Chimica Acta, Zurich, Wiley-VCH, Weinheim
5. Wong E, Giandomenico CM (1999) Chem Rev 99:2451–2466
6. Van Vliet PM (1996) PhD Thesis, Leiden University, The Netherlands
7. Nováková O, Kaspárková J, Vrána O, Van Vliet PM, Reedijk J, Brabec V (1995) Biochemistry 34:12369–12378
8. Velders AH, Kooijman H, Spek AL, Haasnoot JG, de Vos D, Reedijk J (2000) Inorg Chem 39:2966–2967
9. Goswami S, Chakravarty AR, Chakravorty A (1981) Inorg Chem 29:2246–2250

10. Krause RA, Krause K (1980) Inorg Chem 19:2600–2603
11. Velders AH, Van der Schilden K, Hotze ACG, Reedijk J, Kooijman H, Spek AL (2004) J Chem Soc Dalton Trans 448–455
12. Popov AM, Egorova MB, Lutovinov VA, Dmitrieva RI (1990) Zh Obshch Khim 60:2169
13. Goswami S, Mukherjee R, Chakravorty A (1983) Inorg Chem 22:2825–2832
14. Goswami S, Chakravarty AR, Chakravorty A (1983) Inorg Chem 11:602–609
15. Bag N, Pramanik A, Lahiri GK, Chakravorty A (1992) Inorg Chem 31:40–45
16. Ackermann MN, Kiihne SR, Saunders PA, Barnes CE, Stallings SC, Kim HD, Woods C, Lagunoff M (2002) Inorg Chim Acta 334:193–203
17. Ackermann MN, Naylor JW, Smith EJ, Mines GA, Amin NS, Kerns ML, Woods C (1992) Organometallics 11:1919–1926
18. Bao T, Krause K, Krause RA (1988) Inorg Chem 27:759–761
19. Sheldrick GM (1986) SHELXS86 Program for crystal structure determination. University of Göttingen, Germany
20. Sheldrick GM (1997) SHELXL97 Program for crystal structure refinement. University of Göttingen, Germany
21. Sheldrick GM (1996) SHELXL-97 Program for crystal structure refinement. University of Göttingen, Germany
22. Sluis P, Spek AL (1990) Acta Crystallogr A46:194–201
23. Spek AL (1990) Acta Crystallogr A46: C-34
24. Wilson AJC (ed) (1992) International tables for crystallography, vol C. Kluwer, Dordrecht,
25. Boyd MR (1997) In: Teicher, BA (eds) The NCI in vitro anticancer drug discovery system. Humana Press, Totowa, USA, pp 23–42
26. Keepers YP, Pizao PE, Peters GJ, Van Ark-Otte J, Winograd B, Pinedo HM (1991) Eur J Cancer 27:897–900
27. Tada H, Shiho O, Kuroshima K, Koyama M, Tsukamoto K (1986) J Immun Methods 93:156–165
28. Tamura H, Arai T, Nagase M, Ichinose N (1992) Bunseki Kagaku 41: T13–T18
29. Cocchietto M, Sava G (2000) Pharmacol Toxicol 87:193–197
30. Velders AH, Hotze ACG, van Albada GA, Haasnoot JG, Reedijk J (2000) Inorg Chem 39:4073–4080
31. Santra PK, Misra TK, Das D, Sinha C, Slawin AMZ, Woollins JD (1999) Polyhedron 18:2869–2878
32. Lu T-H, Misra TK, Lin P-C, Liao F-L, Chung C-S (2003) Polyhedron 22:535–541
33. Das C, Saha A, Hung CH, Lee GH, Peng SM, Goswami S (2003) Inorg Chem 42:198–204
34. Misra TK, Das D, Sinha C, Ghosh P, Pal CK (1998) Inorg Chem 37:1672–1678
35. Seal A, Ray S (1984) Acta Cryst C40:932
36. Hotze ACG, Bacac M, Velders AH, Jansen BAJ, Kooijman H, Spek AL, Haasnoot JG, Reedijk J (2003) J Med Chem 46:1743–1750
37. Hotze ACG, Velders AH, Ugozzoli F, Biagini-Cingi M, Manotti-Lanfredi AM, Haasnoot JG, Reedijk J (2000) Inorg Chem 39:3838–3844
38. Iwamoto M, Elessio E, Marzilli LG (1996) Inorg Chem 35:2384–2389
39. Velders AH (2000)PhD Thesis, Leiden University, The Netherlands
40. Velders AH, Hotze ACG, Reedijk J J Am Chem Soc: submitted
41. Velders AH, Quiroga AG, Haasnoot JG, Reedijk J (2003) Eur J Inorg Chem: 713–719
42. Flack HD (1983) Acta Crystallogr Sect A A39:876